AJSP
المجلة العربية للنشر العلمي
العدد أربعون
تاريخ الإصدار: 2 – شباط – 2022 م
www.ajsp.net
ISSN: 2663-5798

"Design, Synthesis, QSAR and Molecular Docking of some Substituted Acridinedione Derivatives as Calcium Channel Antagonist"

ResearcherS:

Ahmed Abaker Ahmed Ali[1], Abubaker Mohammed Osman[2], and Ahmed El sadig Mohammed Saeed[3].

[1]Chemistry Department, College of Science and Information Technology, University of Nayala- Nayala- Sudan.
[2]Chemistry Department, College of Science and Atrs (Suratabidha), King Khalid University, Abha, Saudi Arabia.
[3]Chemistry Department, College of Science, Sudan University of Science and Technology- Khartoum- Sudan.

العدد أربعون
تاريخ الإصدار: 2 – شباط – 2022 م
www.ajsp.net
ISSN: 2663-5798

ABSTRACT: In this review, the validation of the model was developed by using LOO method (leave one out method) in order to obtain very good model equation with higher R^2 and very low RMSE value. The statistical quality of the model was also justified by statistical parameters. Molecular docking was also carried out in order to find the good binding affinities of these derivatives with the protein 4gdb. Based upon the QSAR model, a group of acridinedione derivatives were designed and synthesized by the one-pot Hantzsch condensation of an aromatic aldehyde, 5, 5- dimethyl-1, 3-cyclohexanedione (dimedone), and any appropriate amine in refluxing water.

KEYWORDS: Acridinedione Derivatives, QSAR; Docking Studies, Multi-component reactions.

1. Introduction

Quantitative structure activity relationships, often simply known as QSARs, are an analytical application that can be used to interpret the quantitative relationship between the biological activities of a particular molecules and its structure. It is considered a major method of chemical researching all over world today and is frequently used in agricultural, biological, environmental, medicinal, and physical organic studies. Many types of models are possible, with mathematical and statistical models being particularly common. Such models are often referred to as Quantitative Structure-Activity Relationships (QSARs) or Quantitative Structure-Property Relationships (QSPRs) (Tropsha Gramatica et al., 2003). Hansch was the first one to use QSARs to explain the biological activity of series of structurally related molecules (Fujita Iwasa et al., 1964); (Hansch Lien et al., 1968).

Molecular docking of the drug molecule with the receptor (target) gives important information about drug receptor interactions and its commonly used to fine out the binding orientation of drug candidates to their protein targets in order to predict the affinity and activity (Bano Alam et al., 2015).

Hantzsch reported first synthesis of symmetrically substituted 1, 4-dihydropyridine by the one-pot, four-component condensation for two molecules of ethyl acetoacetate, aromatic aldehyde and ammonia (Ghorbani Choghamarani Zolfigol et al., 2008). The standard Hantzsch procedure does not need the intervention of any additive or reagent and the reaction was originally conducted either in acetic acid or at reflux in alcohol for further long periods, resulting in low or modest yields of condensation products (Leov, 1965). Replacement of ammonia by ammonium acetate allowed the efficient synthesis of Hantzsch compounds in aqueous medium as well as under solvent conditions (Wang Xia et al., 2006).

Multi-component Reactions (MCRs) play an important role in combinatorial chemistry because of its ability to synthesized small drug-like molecules with several degrees of structural diversity. A MCR is defined as three or more different starting materials that react to form a product, where most, if not all of the atoms are incorporated in the final product. This reaction tool allows compounds to be synthesized in a few steps and usually in a one-pot operation. Another typical benefit from these reactions is simplified purification, because all of the reagents are incorporated into the final product(Zhu and Bienaymé, 2006).

2. Experimental

2.1. QSAR Study

2.1.1. Data Set

In this QSAR studies, a total of 6 substituted acridinedione derivatives were gathered from. The vitro cytotoxicity of these derivatives was reported against various human cancer cell lines (Hela, MCF-7, LS-180, and Raji cells). The target human cell line in this study is human breast cancer cells (MCF-7 adenocarcinoma cells) (Jamalian Miri et al., 2011) .

The anti-cancer activity which is expressed by the anti-cancer potential (PIC_{50}) is defined

The activity in terms of IC_{50} for training set and IC_{50} for test set compounds was expressed in microgram per milliliter were converted to the negative logarithmic concentration, PIC_{50}), in order to obtain higher mathematical values when the structures are biologically very efficient (Mahama Aboudramane et al., 2020) .

ChemSketch software was used for drawing sets of studied compounds see table (2.1) and (2.2). Then the data sets of the imidazolyl derivatives of 1, 8- acridinediones were divided into two sets, training set (4 compounds) and test set (2), random selection(Jamalian Miri et al., 2011).

Table.1. Structures, IC_{50}, and PIC_{50} of the derivatives of imidazolyl
derivatives of 1, 8-acridinediones, the training sets (Jamalian, Miri et al. 2011):-

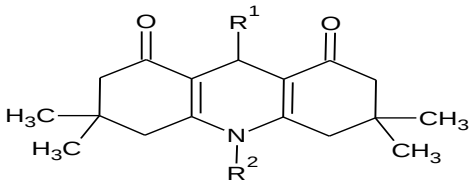

العدد أربعون
تاريخ الإصدار: 2 – شباط – 2022 م
www.ajsp.net
ISSN: 2663-5798

Comp. No	R_1	R_2	IC_{50}	PIC_{50} (exp)	PIC_{50} (pred)*	Res
1/T	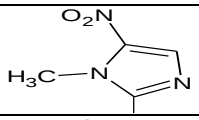	H	31.7	4.5000	4.4944	0.0056
2	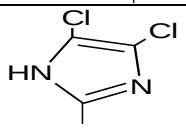	H	54	4.2700	4.2935	-0.0235
3	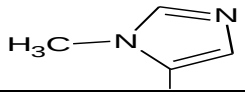	H	100	4.0000	3.9991	0.0009
4	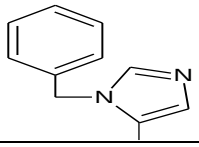	H	54.8	4.2600	4.2429	0.0171
5/T*	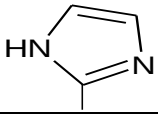	H	10	5.0000	5.00	0.00
6	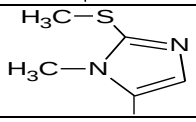	H	25	4.6000	4.60	0.00

T= Training Set T*= Test Set, LOO = Leave one Out. PIC_{50} (pred)* obtained from model No. (3)

2.1.2. Molecular Descriptors

Total of 15 molecular descriptors 2D descriptors, including Mw (Molecular Weight), logP (octanol/water) logP o/w), Mr (Molar refracticity), a-aac (Number of Hydrogen Bond acceptor atoms), a-don (Number of Hydrogen Bond doner atoms), Lip-acc (Lipinski acceptor count), Lip-don (Lipinski donor count), and TPSA (Topological Polar Surface Area). And 3D descriptors such as AMI-IP (Ionization Potential), E (Potential Energy), MNDO-IP (Potential Energy), PM3-IP (Potential Energy), MNDO-Ele (Electronic Energy), MNDO-HF (Heat of Formation), and MNDO-HOMO (Higher Occupied Molecular Orbital Energy), were obtained for the training set and test set in table (2).

Table . 2 illustrated values of descriptors that calculated for training set, and test set compounds

com.No	E	logP(o/w)	MNDO_IP	Mr	PM3_IP	M.wt	AM1-IP	a-acc	a-_don	Lip-acc	Lip-don	MNDO-Eele	MNDO-HF	MNDO-HOMO	TPSA
1/T	47.14	2.50	9.178	10.59	8.94	398.46	8.910	3.00	1.00	8.00	1.00	-995168.18	-1.6203	-9.1778	109.810
2	35.87	3.77	9.072	10.58	8.44	408.33	8.534	4.00	3.00	5.00	2.00	-886186.56	-36.6303	-9.0724	74.8500
3	40.44	2.17	8.747	10.05	8.53	353.47	8.426	3.00	1.00	5.00	1.00	-837239.12	-20.2847	-8.7472	63.9900
4	63.79	4.26	8.576	13.47	8.62	457.62	8.255	3.00	1.00	5.00	1.00	-1180912.2	-4.0609	-8.5760	63.9000
5/T*	35.16	1.78	8.724	9.59	8.70	339.44	8.482	4.00	3.00	5.00	2.00	-780437.25	-22.5276	-8.7243	74.8500
6	52.52	3.16	8.838	11.24	8.77	399.56	8.405	3.00	1.00	5.00	1.00	-945555.68	-21.8426	-883779	63.9900

2.1.3. Model Development

The QSAR model equation with high square of the correlation coefficient (R^2= (0.9930) and low Root Mean Square Error (RMSE = 0.0148) was QSAR model equation(3) :

PIC_{50} =-3.20129+0.15696 * logP(o/w)+0.81590 * AM1-IP. Model No. (1).

PIC_{50} =2.97797+0.13501 * logP(o/w) +0.14800 * lip-acc . Model No. (2).

PIC_{50} = 3.11067+0.11632 * logP(o/w) +0.00995 * TPSA. Model No. (3).

PIC50 = -3.13167 + 0.00363 * Weight + 0.69421* AM1-IP. Model No. (4).

PIC50 =2.58357+0.00252 * Weight+0.00837 *TPSA. Model No. (5).

2.1.4. Validation model.

The validation of the model was developed by using (leave one out) LOO method in order to obtain very good model with higher R^2 and low RMSE value.

2.2. Calculation of Statistical parameters

The statistical quality of the model was justified by statistical parameters such as the root mean square error (RMSE), correlation coefficient (R), square correlation coefficient (R^2), standard error of estimate(S), and (F- test value) or (the ratio between the variances of observed and calculated activities).

Calculation of statistical parameter was carried out by using statistical programme SPSS version IBM-24

Model, R= 0.996, R^2= 0.993 Q= 0.9085, the standard error of estimate = 0.04329,

S = 0.209, F value = 283.74, p value= 0.004, RMSE= 0.124, and Q^2 = 0.990.

3. Results and Discussion

3.1. QSAR Study

Among different derivatives of 1, 4-DHPs, 1, 8- acridinedione is a known scaffold with wide spectrum of biological effects such as anti-malarial activity and DNA active, anti-tumor, and cytotoxic activity (Jamalian Miri et al., 2011).

In this work QSAR study was carried out for Imidazolyl derivatives of 1, 8- Acridinediones. Data set was collected from literature (Jamalian, Miri et al. 2011). Consist of 12 compounds table (2.) and table (2.) which is then divided into two sub set. Training set containing four compounds and test set of two compounds.

All descriptors were calculated by using MOE and ACD/lab programmes. For a statistically reliable model, the number of compounds and number of descriptors should bear a relation of at least 5:1. Thus, only two descriptors are required for 10 compounds in the training set to develop statistically reliable QSAR model. Selection of a set of appropriate descriptors from a large number of them requires a method, which is able to distinguish between the parameters.

QSAR models were developed during MLR analysis in training set with two descriptors and the best equation which showed high square correlation coefficient (R^2) and low root mean square error (RMSE) was considered as the best model with AM1-IP and logP (o/w).

PIC_{50} =-3.20129+0.15696 * logP(o/w)+0.81590 * AM1-IP. Model No. (1).

PIC_{50} =2.97797+0.13501 * logP(o/w) +0.14800 * lip-acc . Model No. (2).

PIC_{50} = 3.11067+0.11632 * logP(o/w) +0.00995 * TPSA. Model No. (3).

PIC50 = -3.13167 + 0.00363 * Weight + 0.69421* AM1-IP. Model No. (4).

PIC50 =2.58357+0.00252 * Weight+0.00837 *TPSA. Model No. (5).

The developed QSAR model equation (model No.3) showed a relationship between in-vitro biological activities and correlated two descriptors TPSA and logP (o/w). It is indicated that from the model equation that the molecular descriptors, namely logP (o/w) partition coefficient and (topological polar surface area), TPSA are positively correlated with PIC_{50}.

4. Designing of acridinedione derivatives

Acridinedione derivatives have attracted attention of medicinal Chemists for both with regard to heterocyclic and the pharmacological activities associated with them. In order to synthesize these derivatives expecting to possess biological activities against breast cancer, about 75 compounds were designed as anti-breast cancer and their predicted biological activities were illustrated in table (3).

The proposed model (3) has all conditions to be considered as predictive model. It has correlation coefficient of cross-validation (Q^2) larger than 0.5, prediction (R^2) which is higher than 0.6 and excellent prediction in external validation (R^2=1). Thus, this model was used to predict the in-vitro biological activity of designed N-substituted acridinedione derivatives from (C1-C75) against human breast cancer Cell Lines MCF-7, predicted biological activity of these compounds along with predicted descriptors were tabulated in table (1). To select compounds for synthesis from designed one, the drugability of these compounds were evaluated through Lipinski‘s parameters rule of five which proposes that molecules with poor permeation and oral absorption have logP>5, molecular weight >500, more than 5 hydrogen-bond donor, and more than 10 acceptor groups.

All designed accridinedione derivatives have acceptable number of hydrogen bond donor and acceptor groups.

The logP value is one of the most important descriptors to evaluate oral bioavailability because which indicates the lipophilicity and hydro solubility of a compound. As much lipophilicity is the compound, as better is the capacity to pass the lipidic-bilayer of the cellular membrane, and consequently, as high will be the bioavailability. The problem is that compounds excessively lipophilicity has difficult to dissolve in the water of organism, and then, it will not be absorbed the molecular weight describes the molecular size. Big molecules will have difficult to be absorbed because, the passage through biological membranes is unfavorable (Yunta, 2017).

The compounds that not passed in this criterion were compounds 34 and 36.

AJSP
المجلة العربية للنشر العلمي
العدد أربعون
تاريخ الإصدار: 2 – شباط – 2022 م
www.ajsp.net
ISSN: 2663-5798

But rest of these compounds are fit in rule of five can be classified as drug-like compounds, these compounds were selected for synthesis, other compounds were selected randomly for synthesis see table (3).
The selected compounds which showed low to high predicted PIC_{50} ranging from 3.60 to4.85compared with (PIC_{50} = 3.84). The rest of selected compounds showed high or low predicted PIC_{50} (3.60 to 4.67), when compared with compound C40.

Table. 3. Designing of some acridinedione derivatives and their predicted PIC_{50}

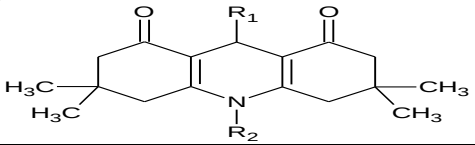

Com No.	R_1	R_2	AM1-IP	a-_acc	a-_don	TPSA	logP(o/w)	Weight	*predicted PIC_{50}
C1	H	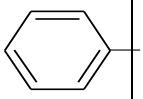	8.2156	2	0	37.38	4.347	349.47	3.99
C2	CH_3	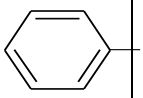	8.3064	2	0	37.38	4.717	363.50	4.03
C3	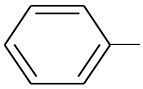	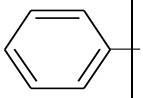	8.4354	2	0	37.38	5.992	425.57	4.18
C4	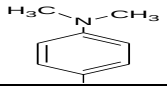	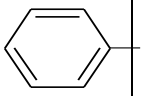	7.9581	2	0	40.62	5.907	468.64	4.20
*C5	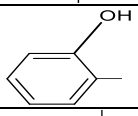	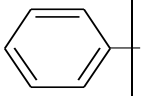	8.4654	3	1	57.61	5.721	441.57	4.34
*C6	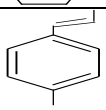	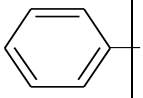	8.4154	2	0	37.38	6.636	451.61	4.25
C7	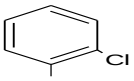	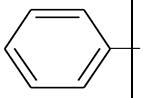	8.3442	2	0	37.38	6.582	460.01	4.25
C8	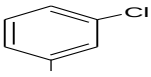	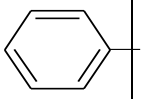	8.6348	2	0	37.8	6.621	460.01	4.25
C9	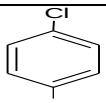	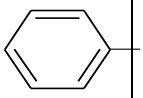	8.4972	2	0	37.38	6.584	460.01	4.25
C10	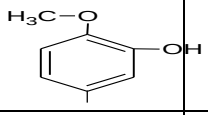	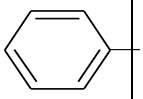	8.3644	4	1	66.81	5.675	471.59	4.44
C11	H	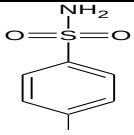	8.4572	4	1	97.54	2.775	428.55	4.40
C12	CH_3		8.5476	4	1	97.54	3.145	442.58	4.45

		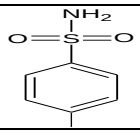							
C13	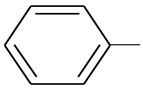	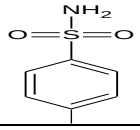	8.6418	4	1	97.54	4.42	504.65	4.60
*C14	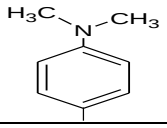	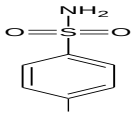	8.0675	4	1	100.78	4.335	547.72	4.62
*C15	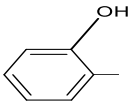	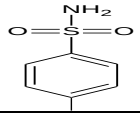	8.7304	5	2	117.77	4.149	520.65	4.77
*C16	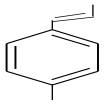	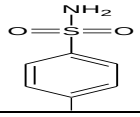	8.6884	4	1	97.54	5.064	530.68	4.67
C17	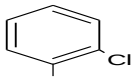	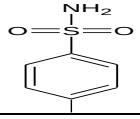	8.6583	4	1	97.54	5.01	539.09	4.66
C18	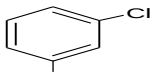	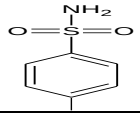	8.7366	4	1	97.54	5.049	539.09	4.67
C19	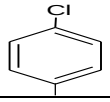	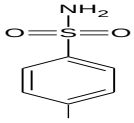	8.7937	4	1	97.54	5.012	539.09	4.66
C20	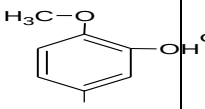	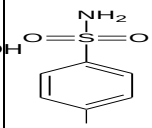	8.5620	6	2	127.00	4.103	550.67	4.85

*predicted (PIC_{50}) were calculated from QSAR model equation, No. (3).
*Based upon the QSAR model, and molecular docking the following compounds *5, *C6, *C14, *C15, and *C16 were selected for synthesis.

العدد أربعون
تاريخ الإصدار: 2 – شباط – 2022 م
www.ajsp.net
ISSN: 2663-5798

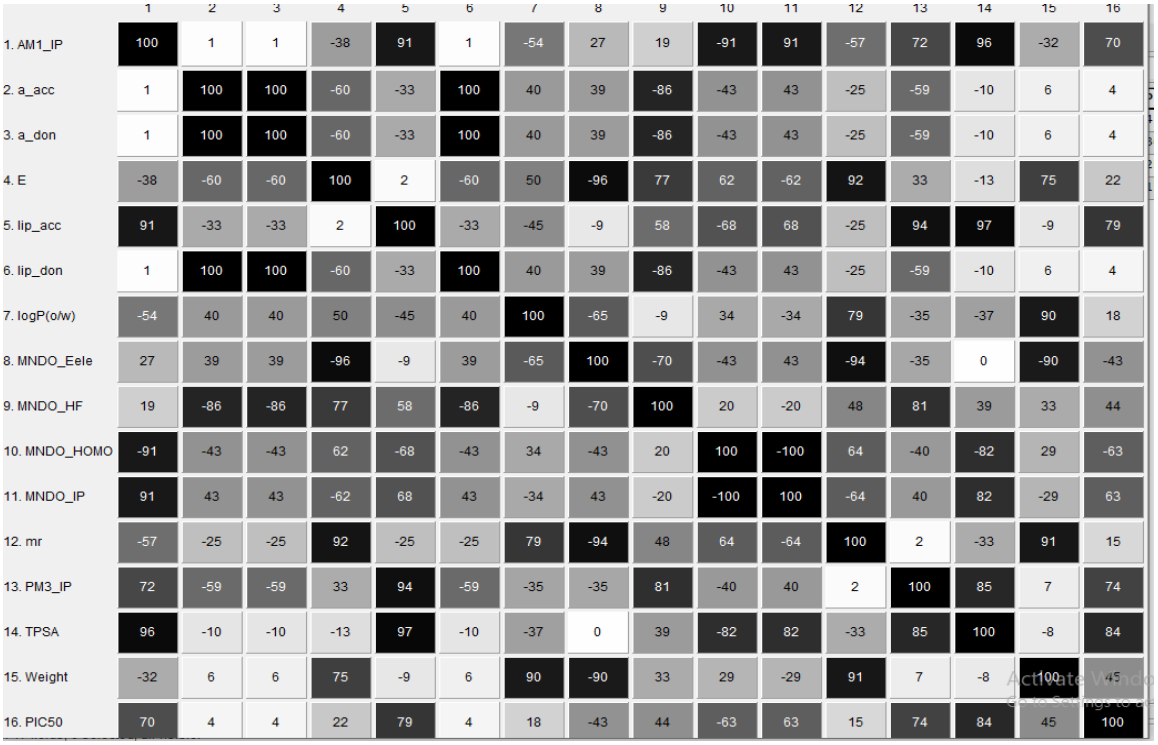

	1	2	3	4	5	6	7	8	9	10	11	12	13	14	15	16
1. AM1_IP	100	1	1	-38	91	1	-54	27	19	-91	91	-57	72	96	-32	70
2. a_acc	1	100	100	-60	-33	100	40	39	-86	-43	43	-25	-59	-10	6	4
3. a_don	1	100	100	-60	-33	100	40	39	-86	-43	43	-25	-59	-10	6	4
4. E	-38	-60	-60	100	2	-60	50	-96	77	62	-62	92	33	-13	75	22
5. lip_acc	91	-33	-33	2	100	-33	-45	-9	58	-68	68	-25	94	97	-9	79
6. lip_don	1	100	100	-60	-33	100	40	39	-86	-43	43	-25	-59	-10	6	4
7. logP(o/w)	-54	40	40	50	-45	40	100	-65	-9	34	-34	79	-35	-37	90	18
8. MNDO_Eele	27	39	39	-96	-9	39	-65	100	-70	-43	43	-94	-35	0	-90	-43
9. MNDO_HF	19	-86	-86	77	58	-86	-9	-70	100	20	-20	48	81	39	33	44
10. MNDO_HOMO	-91	-43	-43	62	-68	-43	34	-43	20	100	-100	64	-40	-82	29	-63
11. MNDO_IP	91	43	43	-62	68	43	-34	43	-20	-100	100	-64	40	82	-29	63
12. mr	-57	-25	-25	92	-25	-25	79	-94	48	64	-64	100	2	-33	91	15
13. PM3_IP	72	-59	-59	33	94	-59	-35	-35	81	-40	40	2	100	85	7	74
14. TPSA	96	-10	-10	-13	97	-10	-37	0	39	-82	82	-33	85	100	-8	84
15. Weight	-32	6	6	75	-9	6	90	-90	33	29	-29	91	7	-8	100	45
16. PIC50	70	4	4	22	79	4	18	-43	44	-63	63	15	74	84	45	100

Figure.1. Details of correlation matrix for molecular descriptors in training set compounds, acridinedione derivatives.

Internal validation by training set Validation is a crucial aspect of any QSAR analysis, this step achieved by set compounds (cross validation) and external validation by test set compounds.

The statistical fit of a QSAR can be assessed in many easily available statistical terms. The statistical quality of the resulting model, as tabulated in table (2.), is determined by R, R^2, Q, Q^2, RMSE, S, F, and P value.

The Square Correlation Coefficient, (R^2) which gives an evaluation of the dispersion of theoretical values around the experimental data. The quality of the model is improved when the points are close to the fitting line, that means if R^2 value closes to 1 the theoretical and experimental values will be assumed to correlate.

Cross-Validation Q^2 is the one of most extensively employed methods for the internal validation of a statistical model is estimated using a reduced set of structural data. Usually, one element of the set is extracted each time, and a new model is derived based on the reduced dataset, which is then employed to predict the activity of the excluded molecule.

Root Mean Square Error (RMSE) has been used as a statistical metric to measure model performance in meteorology, air quality, and climate research studies (Chai and Draxler, 2014). The lower its value the better the model.

The QSAR model represents robustness, with good internal and external predictive capabilities and this model is acceptable because all the values of statistical measures are found to be in the acceptable ranges, the training set compounds:

R=0.996	R^2 =0.993	RMSE=0.124	Q=0. 3963
Q^2 = 0.990	s= 0.209	F= 283.74	p= 0.004

One of the important characteristics of a QSAR model is its predictive power, (the ability of a model to predict accurately the biological activity of the compounds that were not is used for model development (external validation). Whereas, internal validation techniques described above can be used to establish model robustness, they do not directly assess model predictivity. In principle, external validation is the only way to determine the true predictive power of a QSAR model. This type of assessment requires the use of an external test set, compounds which not used for the model development.

The predictivity of a regression model was estimated by comparing the predicted and observed experimental values of PIC_{50} against breast cancer of training set and their cross-validation, the residual values were calculated and listed in table (1) and (2)

AJSP
المجلة العربية للنشر العلمي
العدد أربعون
تاريخ الإصدار: 2 – شباط – 2022 م
www.ajsp.net
ISSN: 2663-5798

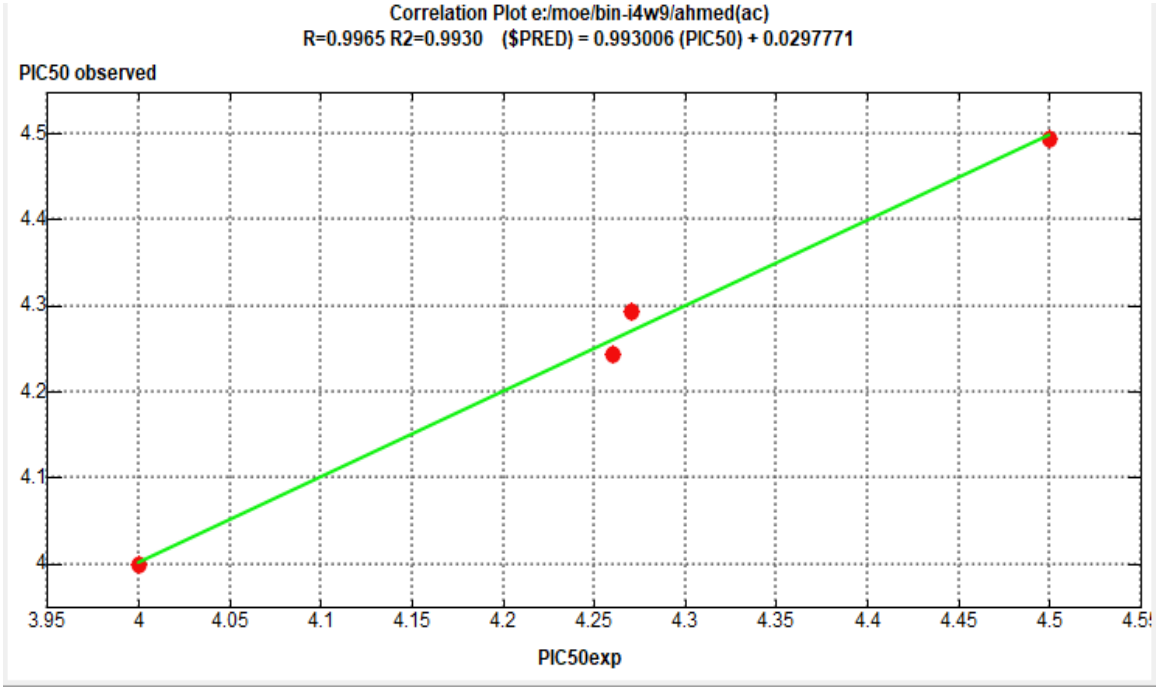

Figure.2. The plot of linear regression predicted PIC_{50} versus experimental values of the biological activity of training set compounds (validation) against human breast cancer MCF-7 Cell Lines.

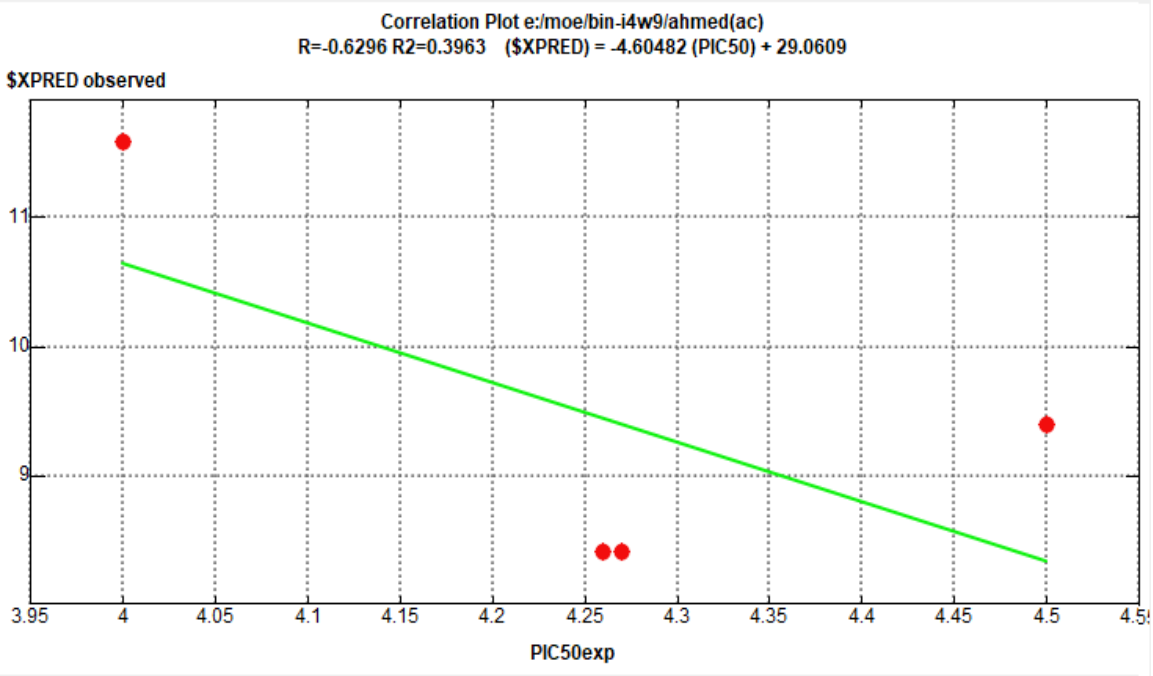

Figure. 3. The plot of linear regression predicted PIC_{50} versus experimental values of the biological activity of training set compounds (cross-validation),

العدد أربعون
تاريخ الإصدار: 2 – شباط – 2022 م
www.ajsp.net
ISSN: 2663-5798

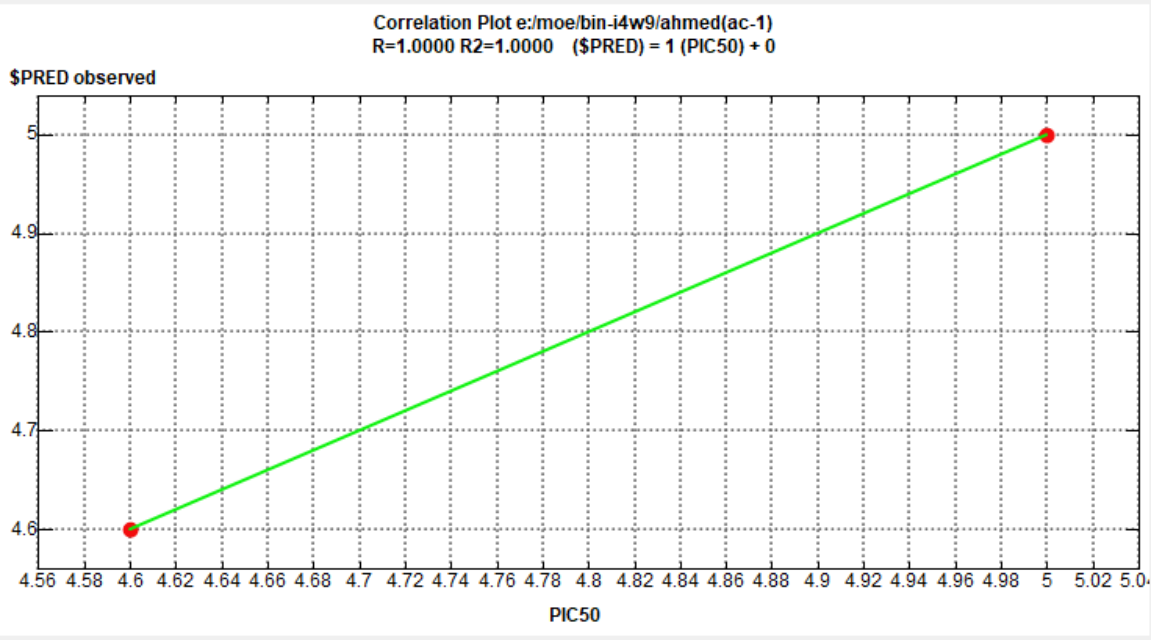

Figure .4. The plot of linear regression predicted PIC_{50} versus experimental values of the biological activity of test set compounds (validation)

The plots for QSAR model shows a good fit with R=0.9661 and R^2 which equal to 0.9334. And Q= 0.9085 Q^2 =0.8253 cross-validation for training set compounds.

And the plots for QSAR in the test set show a good fit with R= 1, R^2 =1(validation).

Table .5. Structures, molecular docking of imidazolyl derivatives of 1, 8-acridinediones, the training sets (Jamalian, Miri et al. 2011) :-

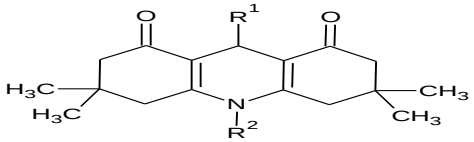

Entry	R1	R2	S	rmsd	Amino - acid	Group of interaction	Types of interaction	Length in (Å)
1	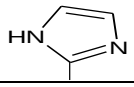	H	50.14	1.36	GluA278 TrpA256	N-H	H-bond	2.02
2	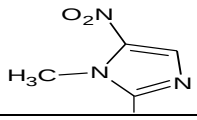	H	79.23	2.45	GluA278 GlnA242 PheA277	N-H N Imidazolyl ring	H-bond π- bond π- bond	2.30 2.81 -
3	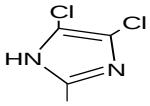	H	38.48	1.26	TrpA386 GluA278 TrpA386 PheA277	C=O N-H Imidazolyl ring Imidazolyl ring	H-bond H-bond π- bond π- bond	2.71 1.72 - -

العدد أربعون
تاريخ الإصدار: 2 – شباط – 2022 م
www.ajsp.net
ISSN: 2663-5798

4	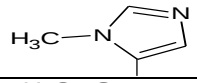	H	16.14	1.40	GluA278	N-H	H-bond	1.82
5	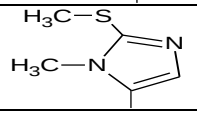	H	11.82	1.16	GluA278	N-H	H-bond	1.88
6	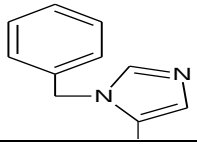	H	12.55	2.36	GluA278	N-H	H-bond	1.80
Doxorubicin (a reference drug)		-35.2941			LeuA280 PheA277 GlnA242 PheA277 TrpB386	N-H N-H OH	H-bond H-bond H-bond π- bond π- bond	2.41 1.88 2.15 - -

Table. 6. Molecular docking of some acridinedione derivatives

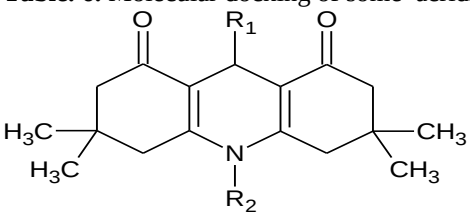

Entry	R1	R2	S	rmsd	Amino - acid	Group of interaction	Types of interaction	Length in (Å)
C1	H	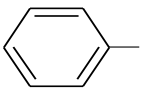	39.89	139	AsnB383 TrpB388	C=O Phenyl	H-bond π- bond	3.23 -
C2	CH_3	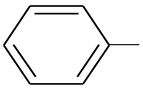	51.68	1.40	SerA274	C=O	H-bond	2.97
C3	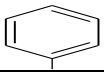	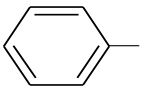	69.36	1.68	GlnA242 TrpB388	C=O Phenyl	H-bond π- bond	2.76 -
C4	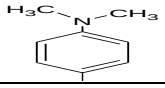	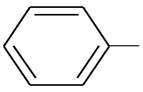	65.01	2.62	AsnB383 TrpB388	C=O Phenyl	H-bond π- bond	2.73 -
C5	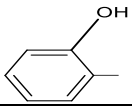	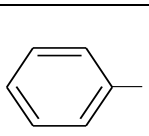	69.12	1.55	AsnB383 GlnA242 TrpB388	C=O C=O Phenyl	H-bond H-bond π- bond	2.77 3.75 -
C6	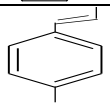	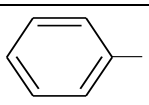	50.17	1.48	TrpB388 PheA277	Phenyl Phenyl	π- bond π- bond	- -
C7	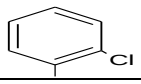	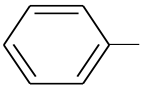	76.29	2.26	SerA274 TrpB388 PheA277	C=O Phenyl Phenyl	H-bond π- bond π- bond	3.16 - -

C8	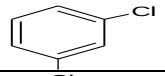	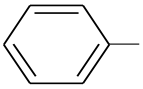	68.81	1.98	AsnB383 GlnA242 TrpB388	C=O C=O Phenyl	H-bond H-bond π- bond	3.73 2.86 -
C9	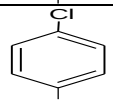	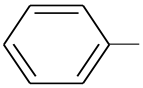	59.91	1.36	TrpB388 PheA277	Phenyl Phenyl	π- bond π- bond	- -
C10	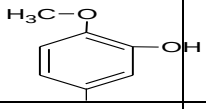	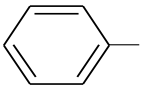	67.82	2.19	GlnA242 AsnB383 TrpB388	C=O C=O Phenyl	H-bond H-bond π- bond	2.73 5.05 -
C11	H	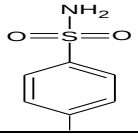	36.69	2.87	SerA274 TrpB388	S=O Phenyl	H-bond π- bond	2.85 -
C12	CH_3	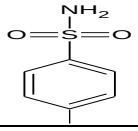	161.73	1.32	GlnA242 AspB383 PheA277 TrpB388	S=O S=O Phenyl Phenyl	H-bond H-bond π- bond π- bond	2.86 3.67 - -
C13	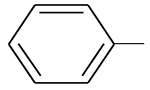	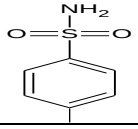	59.55	1.49	SerA274 GlnA242 TrpB388	S=O C=O Phenyl	H-bond H-bond π- bond	2.85 3.84 -
C14	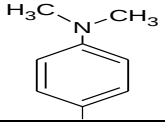	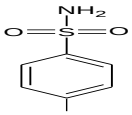	55.92	1.99	SerA274 GlnA242 TrpB388	N-H C=O Phenyl	H-bond H-bond π- bond	2.23 2.74 -
C15	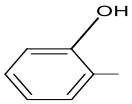	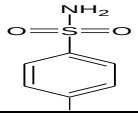	70.41	1.84	GlnA242 SerA274 TrpB388	O-H S=O Phenyl	H-bond H-bond π- bond	2.74 3.02 -
C16	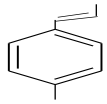	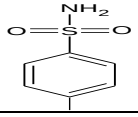	-17.49	6.42	TrpB388 PheA277 LeuA280	Phenyl Phenyl N-H	π- bond π- bond H-bond	- - 2.19
C17	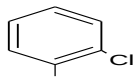	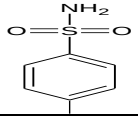	-19.16	9.03	PheA277	Phenyl	π- bond	-
C18	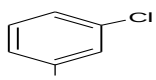	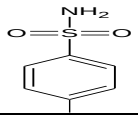	73.71	2.87	AsnB383 SerA277 TrpB388	S=O C=O Phenyl	H-bond H-bond π- bond	3.41 2.70 -
C19			67.38	1.66	AsnB383 GlnA242 SerA274 TrpB388	C=O C=O S=O Phenyl	H-bond H-bond H-bond π- bond	2.86 2.72 2.67 -

AJSP
المجلة العربية للنشر العلمي
العدد أربعون
تاريخ الإصدار: 2 – شباط – 2022 م
ISSN: 2663-5798
www.ajsp.net

	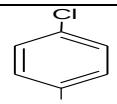	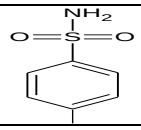						
C20	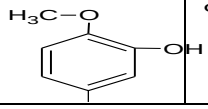	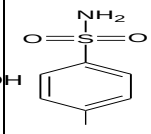	80.51	1.37	SerA274 GluA278 SerA274 TrpB388	O-H O-H CH_3O phenyl	H-bond H-bond H-bond π- bond	3.19 1.76 2.90 -

5. Organic Synthesis

5.1. General procedures. Reagents and solvents were obtained from commercial sources and were not further purified before use. All melting points were uncorrected. Infrared spectra were recorded in KBr pellet and reported in cm^{-1} ^{1}H-NMR spectra were recorded at 850 MHz by using $CDCl_3$ as solvent and reported in parts per million (ppm).

5.1.1. General procedure for the preparation of N- substituted – 3, 3, 6, 6- tetramethylhexahydroacridine-1, 8- Dione derivatives 1a-----2a

A mixture of aldehyde (1mmol), 5, 5-dimethyl-1, 3-cyclohexanedione (dimedone, 2mmol), sulfanilamide (1mmol) and Cetyl trimethyl ammonium bromide (CTAB) (0.1 mmol) in water (4ml) was vigorously stirred under reflux at 85^{0}C, for 6 hours. The workup procedure involved simple filteration and washing twice with water (10ml). The desired product of high purity was further achieved by recrystalization from an aqueous ethanol.

5.1.2. General procedure for the preparation of N- substituted – 3, 3, 6, 6- tetramethylhexahydroacridine-1, 8- Dione derivatives 3a-----5a

A mixture of aromatic aldehyde (1mmol), 5, 5-dimethyl, 1, 3-cyclohexanedione (dimedone, 2 mmol), Aniline, (1mmol) in water (4ml) equipped in round-bottomed flask fitted in refluxed condenser, the reaction mixture was stirred vigorously under reflux for three hours at degree of temperature about 98^{0}C. The reaction mixture was then completed after this period of time, as monitored by using TLC, the workup procedure involved simple filtration and washing cold ice water (10ml). The obtained pale yellow solid product of high purity was further achieved by recrystallization from aqueous ethanol.

Acridinedione derivatives were synthesized by the one-pot three-component Hantzch condensation for a designated time of appropriate aromatic aldehyde, dimedone(5,5- dimethyl-1,3- cyclohexanedione) and appropriate aromatic amines in refluxing water with in the presents of CTAB as a catalyst.

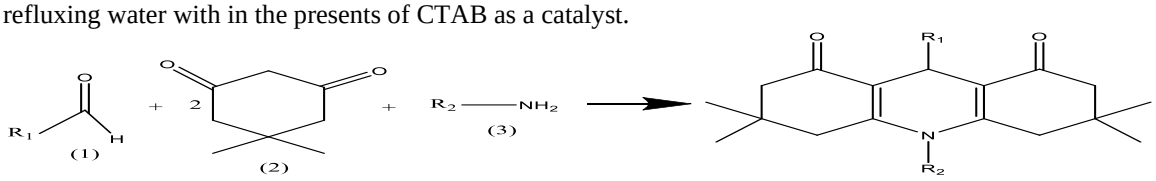

1a----------5a

R_1	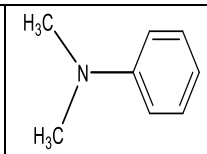	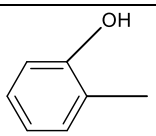	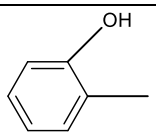	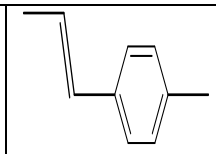	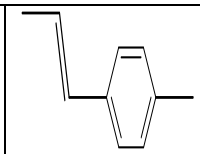
R_2	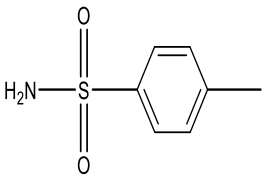	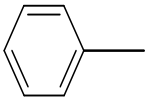	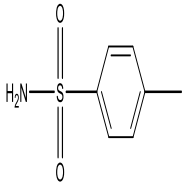	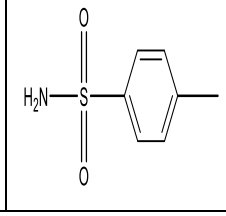	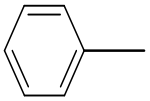

Scheme 1 Synthesis of acridine-1,8- dione derivatives (1a-5a).

The reaction yield of sulfanilamide/ salicylaldehyde compound(3a) is higher than for N, N- dimethyl benzaldehyde, compound(1a) this is due to the presents of the catalyst, and in water due to the solubility.

6. Spectroscopic Analysis

AJSP
المجلة العربية للنشر العلمي
العدد أربعون
تاريخ الإصدار: 2 – شباط – 2022 م
ISSN: 2663-5798
www.ajsp.net

6.1. 4-(9-(4-(dimethylamino)phenyl)-3,3,6,6-tetramethyl-1,8-dioxo-2,3,4,5,6,7,8,9-octahydroacridin-10(1H)-yl) benzenesulfonamide**(1a)**: colour: yellow, yield%= 62, MP= 200- 202 ºC, M.wt= 547, R_f= 0.92. IR(KBr): N-H st.vib, 3446 cm^{-1}, C-H Aliph, 2960 cm^{-1}, OH (bonded), range 3200-3500 cm^{-1},
^{1}H-NMR($CDCl_3$ (CH_3 ,6H,s), 0.0967-1.099; (CH_2), 2.27; (CH_2), 2.32; (CH_3 ,6H,m), 2.46; (CH, 1H), 5.47; Phenyl ring, (4Hq), 7.38-7.059; Phenyl ring, (4Hq), 7.136-7.74; (2H, $NH_{2,S}$), 6.98.
6.2. 9-(2-hydroxyphenyl)-3,3,6,6-tetramethyl-10-phenyl-3,4,6,7,9,10-hexahydroacridine-1,8(2H,5H)-dioned**(2a)**: colour: pale yellow, Y%= 88.9, MP= 183-185 ºC, M.wt= 441, R_f= 0.90.
IR(KBr): C-H Aliph, 2954 cm^{-1}; C=O, 1640 cm^{-1} ; C=C, 1588 cm^{-1} ; OH (bonded) , range 3200-3500 cm^{-1} ;
^{1}H-NMR($CDCl_3$ (CH_3 ,6H,s), 0.86-1.132; (CH_2), 2.02; (CH_2), 2.23; (CH, 1H), 5.108; Phenyl ring, (3Hq); 7.012-7.184; Phenyl ring, (4Hq), 7.410-7.517; OH(1H), 9.926.
6.3.4-(9-(2-hydroxyphenyl)-3,3,6,6-tetramethyl-1,8-dioxo-2,3,4,5,6,7,8,9-octahydroacridin-10(1H)-yl)benzenesulfonamide**(3a):** Colour, yellow, Y%= 92.7%, MP= 185-187 ºC, M.wt = 451, R_f = 0.80.
IR(KBr): N-H st.vib, 3192 cm^{-1} ; OH (bonded), range 3200-3500 cm^{-1}; C=O, 1641 cm^{-1}; ; C=C, 1590 cm^{-1}.
^{1}H-NMR($CDCl_3$ (CH_3 ,6H,s), 1.14-1.32; (CH_2), 2.05-2.13; (CH_2), 2.22-2.63; (CH, 1H), 4.69; Phenyl ring, (4Hq), 7.039-7.17; Phenyl ring, (4Hq), 7.168-7.28; OH(1H), 11.353; (2H, NH_2), 6.942.
6.4.E)-4-(3,3,6,6-tetramethyl-1,8-dioxo-9-styryl-2,3,4,5,6,7,8,9-octahydroacridin-10(1H)-yl)benzenesulfonamide**(4a)**: Colour: pale yellow, Y%= 86.7%, MP= 192-194 ºC, M.wt= 520, R_f= 0.60.
IR(KBr): N-H st.vib, 3367 cm^{-1} ; C-H, 2928 cm^{-1}; ; C=O, 1604 cm^{-1} ; ^{1}H-NMR($CDCl_3$ (CH_3 ,6H,s), 0.899-1.099; (CH_2), 2.123-2.160; (CH_2), 2.22-2.86; (CH, 1H), 3.936;
(CH, 1H), 5.270; (CH, 1H), 6.545; Phenyl ring, (5H,m), 7.132-7.284; Phenyl ring, (4H,q), 7.617-7.73; (2H, NH_2), 6.76.
6.5.(E)-3,3,6,6-tetramethyl-10-phenyl-9-styryl-3,4,6,7,9,10-hexahydroacridine-1,8(2H,5H)-dione **(5a)**: Colour: yellow, Y%=90.9%, MP= 179-180 ºC, M.wt= 530, R_f= 0.67.
IR(KBr): C-H, 2964 cm^{-1}; C=O, 1616 cm^{-1} ; ^{1}H-NMR($CDCl_3$ (CH_3 ,6H,s), 0.932-1.016; (CH_2), 1.185-1.188; (CH_2 1.197-1.244; (CH, 1H), 1.185; (CH, 1H), 2.191; (CH, 1H), 2.304; Phenyl ring, (5H,m), 7.128-7.316; Phenyl ring, (5H,m), 7.323-7.403.

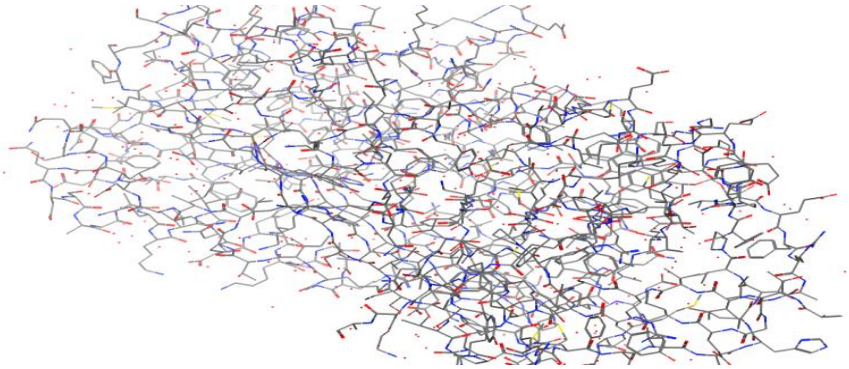

Figure. 5. Showed the3D structure of 5OM7 that was imported from PDB.

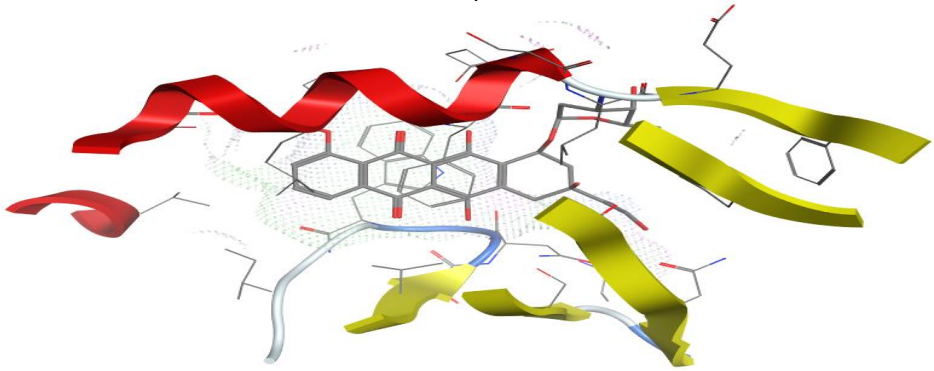

Figure. 6. Showed the structure of 5OM7 pocket after preparation and 2D and 3D, interaction of doxorubicin inside the active site of 5OM7 protein.

العدد أربعون
تاريخ الإصدار: 2 – شباط – 2022 م
www.ajsp.net
ISSN: 2663-5798

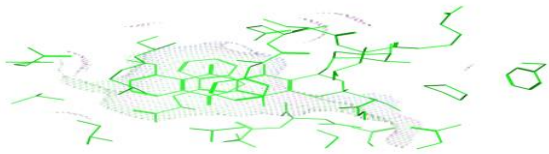

Figure .7. Showed the structure of 5OM7 pocket and ligand after preparation and 2D and 3D, interaction of doxorubicin inside the active site of 5OM7 protein.

Docking on the active site of 5OM7 was performed for all synthesized derivatives of acridinedione and polyhydroquinoline; the results were tabulated in table (4.2) and table (2.10).Compounds of Acridinediones showed low docking scores which ranging from -12.3358 to -13.0118 kcal/mol comparing with compounds that carrying sulfonanilamide moiety which showed proper fitting to the active site of 5OM7 with high energy scores

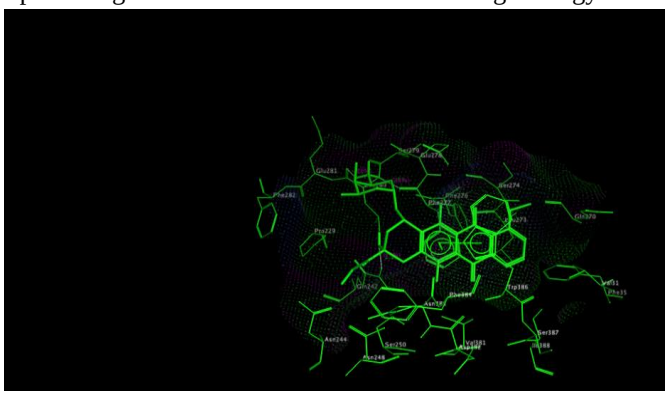

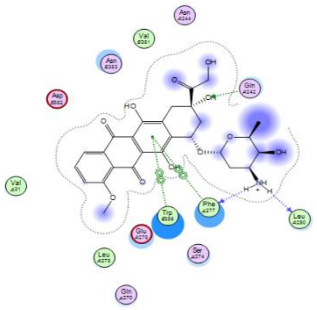

Figure.8. Showed 3D and 2D, interaction of doxorubicin inside the active site of 5OM7 protein.

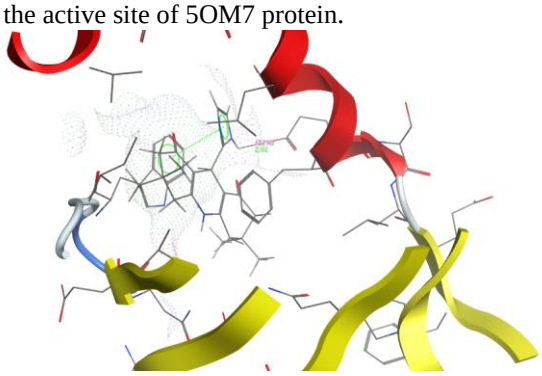

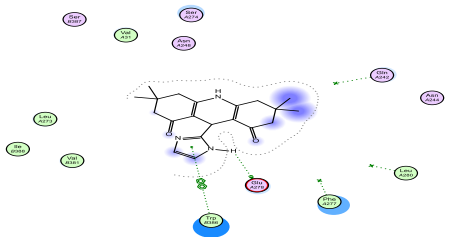

Figure.9. Showed 3D and 2D, interaction of 9-(1H-imidazol-2-yl)-3,3,6,6-tetramethyl-3,4,6,7,9,10-hexahydroacridine-1,8(2H,5H)-dione(1) inside the active site of 5OM7 protein.

العدد أربعون
تاريخ الإصدار: 2 – شباط – 2022 م
www.ajsp.net
ISSN: 2663-5798

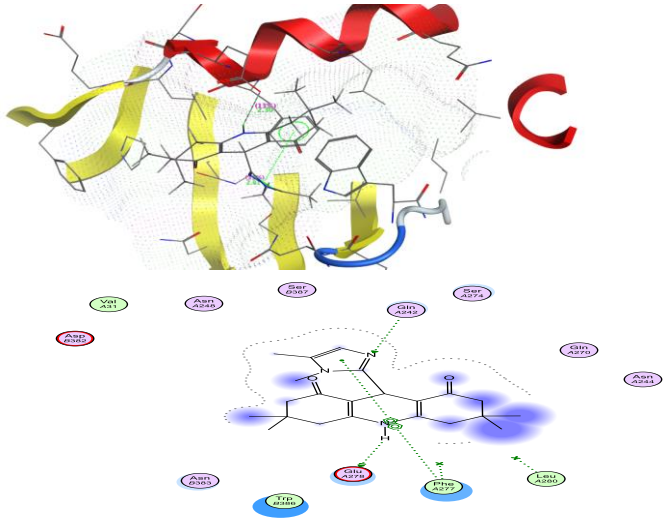

Figure.10. Showed 3D and 2D, interaction of 9-(1,5-dimethyl-1H-imidazol-2-yl)-3,3,6,6-tetramethyl-3,4,6,7,9,10-hexahydroacridine-1,8(2H,5H)-dione (2) inside the active site of 5OM7 protein.

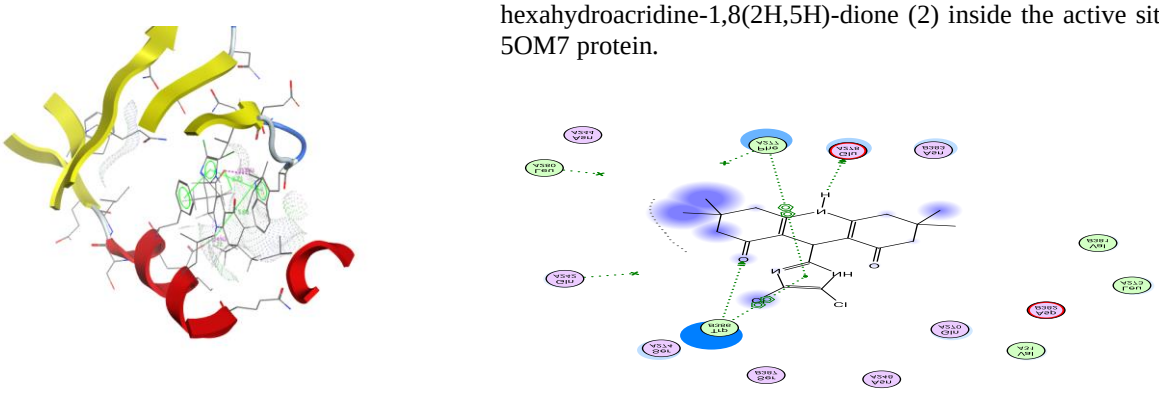

Figure.11. Showed 3D and 2D, interaction of 9-(4,5-dichloro-1H-imidazol-2-yl)-3,3,6,6-tetramethyl-3,4,6,7,9,10-hexahydroacridine-1,8(2H,5H)-dione(3) inside the active site of 5OM7 protein.

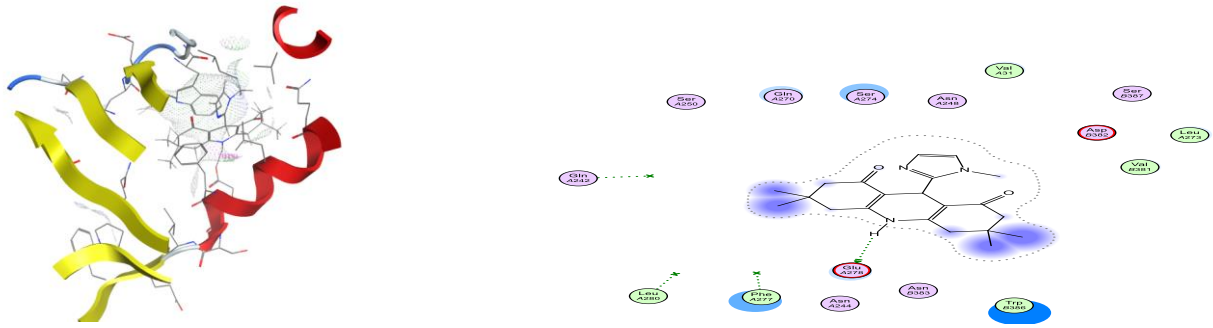

Figure.12. Showed 3D and 2D, interaction of 3,3,6,6-tetramethyl-9-(1-methyl-1H-imidazol-2-yl)-3,4,6,7,9,10-hexahydroacridine-1,8(2H,5H)-dione(4) inside the active site of 5OM7 protein.

AJSP
المجلة العربية للنشر العلمي
العدد أربعون
تاريخ الإصدار: 2 – شباط – 2022 م
www.ajsp.net
ISSN: 2663-5798

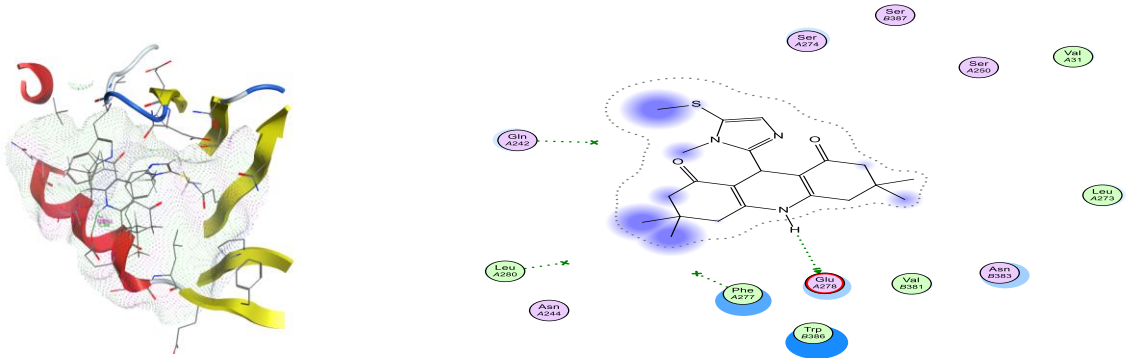

Figure.13. Showed 3D and 2D, interaction of 3,3,6,6-tetramethyl-9-(1-methyl-5-(methylthio)-1H-imidazol-2-yl)-3,4,6,7,9,10-hexahydroacridine-1,8(2H,5H)-dione(5) inside the active site of 5OM7 protein.

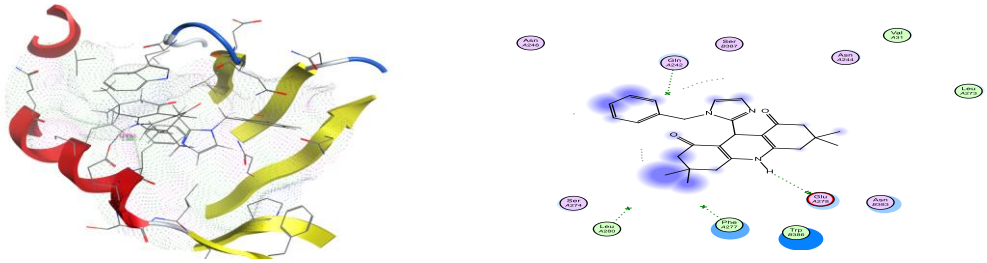

Figure.14. Showed 3D and 2D, interaction of 9-(5-benzyl-1H-imidazol-2-yl)-3,3,6,6-tetramethyl-3,4,6,7,9,10-hexahydroacridine-1,8(2H,5H)-dione(6) inside the active site of 5OM7 protein.

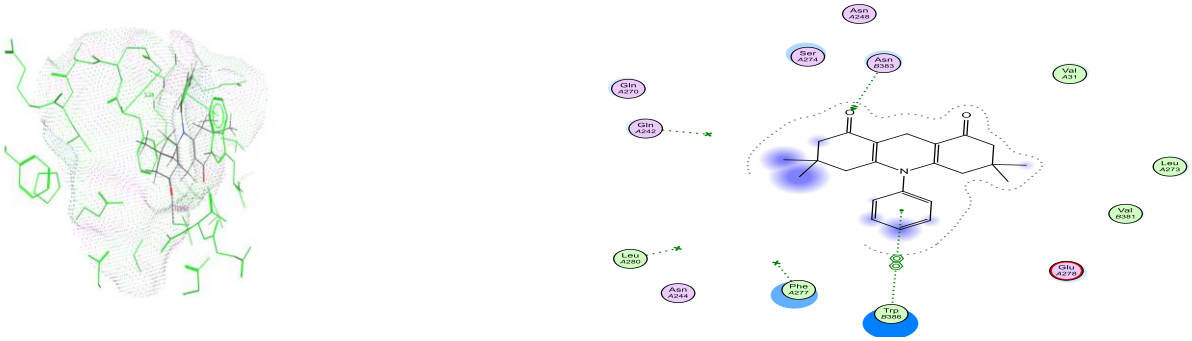

Figure 15. Showed 3D and 2D, interaction of C1/ 3,3,6,6-tetramethyl-10-phenyl-3,4,6,7,9,10-hexahydroacridine-1,8(2H,5H)-dione inside the active site of 5OM7 protein.

العدد أربعون
تاريخ الإصدار: 2 – شباط – 2022 م
www.ajsp.net
ISSN: 2663-5798

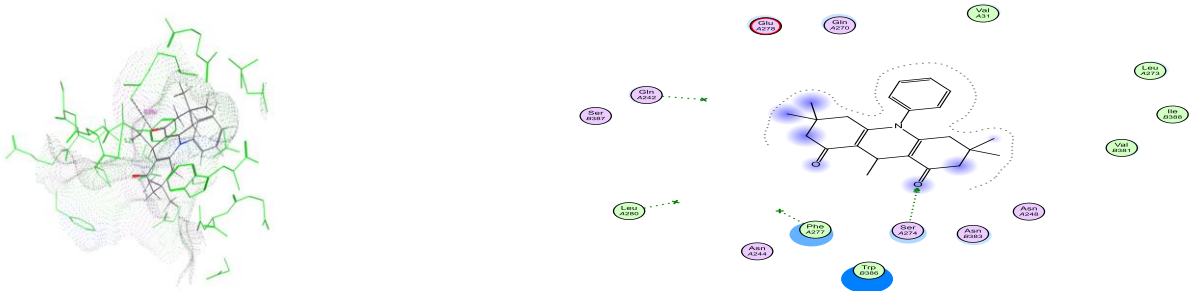

Figure 16. Showed 3D and 2D, interaction of C2/ 3,3,6,6,9-pentamethyl-10-phenyl-3,4,6,7,9,10-hexahydroacridine-1,8(2H,5H)-dione inside the active site of 5OM7 protein.

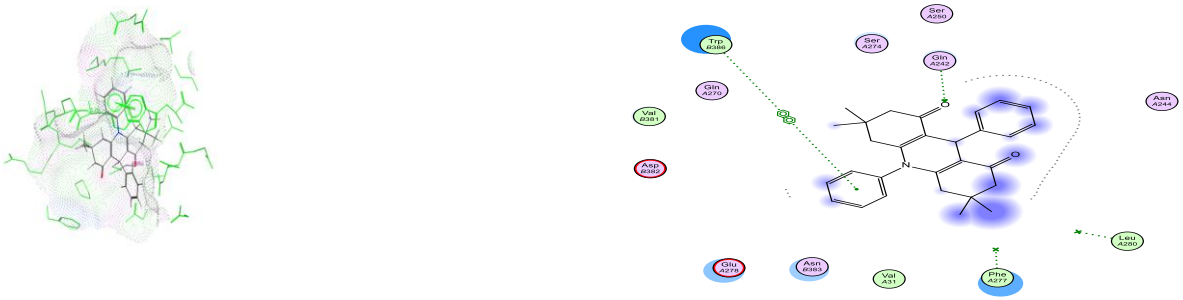

Figure 17. Showed 3D and 2D, interaction of C3/ 3,3,6,6-tetramethyl-9,10-diphenyl-3,4,6,7,9,10-hexahydroacridine-1,8(2H,5H)-dione inside the active site of 5OM7 protein.

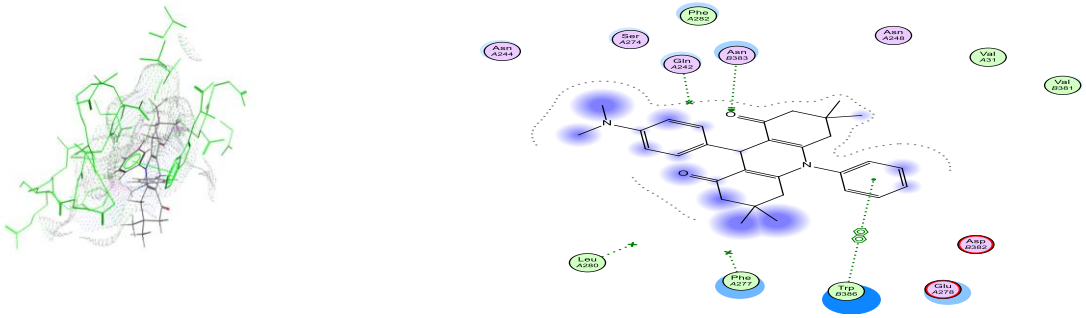

Figure 18. Showed 3D and 2D, interaction of C4/ 9-(4-(dimethylamino)phenyl)-3,3,6,6-tetramethyl-10-phenyl-3,4,6,7,9,10-hexahydroacridine-1,8(2H,5H)-dione inside the active site of 5OM7 protein.

العدد أربعون
تاريخ الإصدار: 2 – شباط – 2022 م
www.ajsp.net
ISSN: 2663-5798

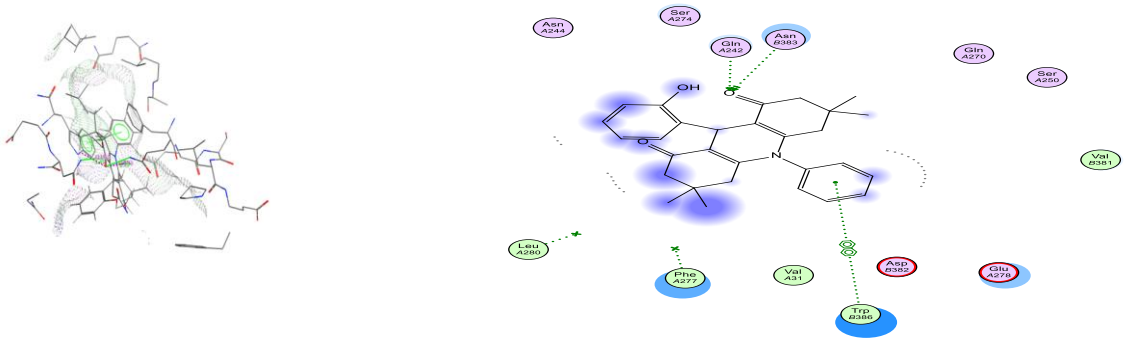

Figure 19. Showed 3D and 2D, interaction of C5/ 9-(2-hydroxyphenyl)-3,3,6,6-tetramethyl-10-phenyl-3,4,6,7,9,10-hexahydroacridine-1,8(2H,5H)-dione inside the active site of 5OM7 protein.

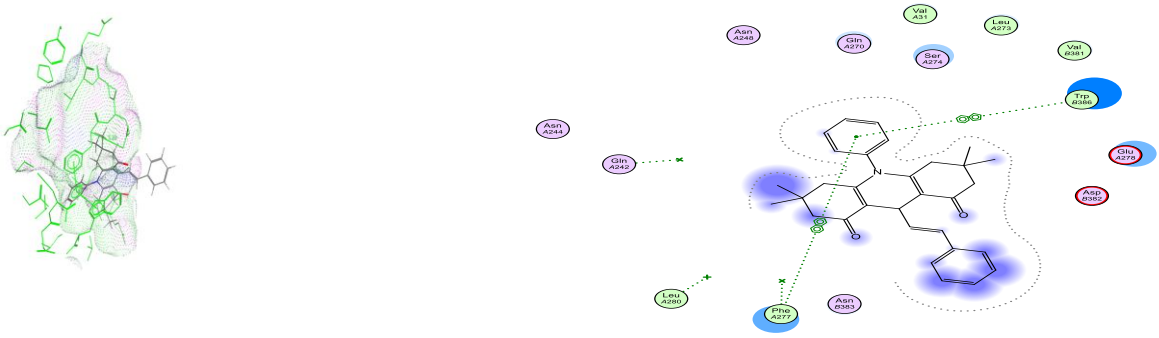

Figure 20. Showed 3D and 2D, interaction of C6/ (E)-3,3,6,6-tetramethyl-10-phenyl-9-styryl-3,4,6,7,9,10-hexahydroacridine-1,8(2H,5H)-dione inside the active site of 5OM7 protein.

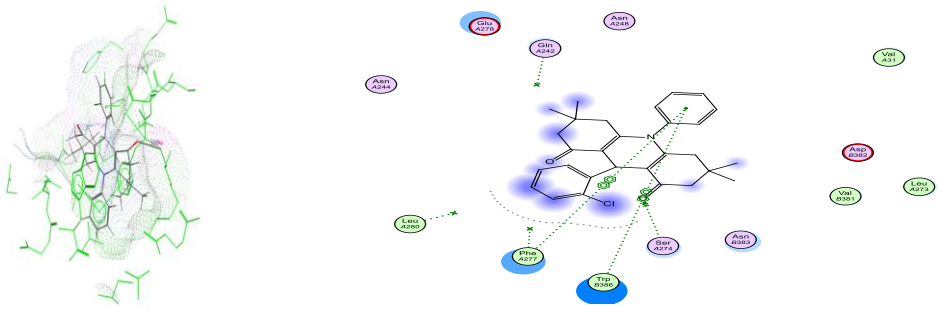

Figure 21. Showed 3D and 2D, interaction of C7/ 9-(2-chlorophenyl)-3,3,6,6-tetramethyl-10-phenyl-3,4,6,7,9,10-hexahydroacridine-1,8(2H,5H)-dione inside the active site of 5OM7 protein.

AJSP
المجلة العربية للنشر العلمي
العدد أربعون
تاريخ الإصدار: 2 – شباط – 2022 م
www.ajsp.net
ISSN: 2663-5798

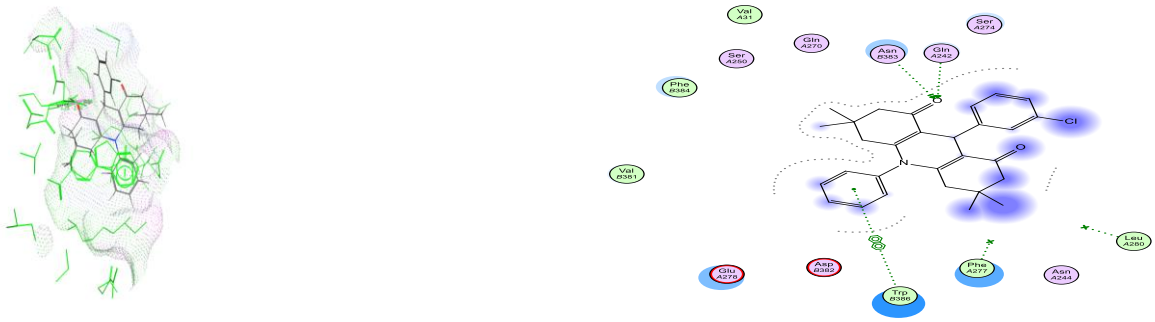

Figure 22. Showed 3D and 2D, interaction of C8/ 9-(3-chlorophenyl)-3,3,6,6-tetramethyl-10-phenyl-3,4,6,7,9,10-hexahydroacridine-1,8(2H,5H)-dione inside the active site of 5OM7 protein.

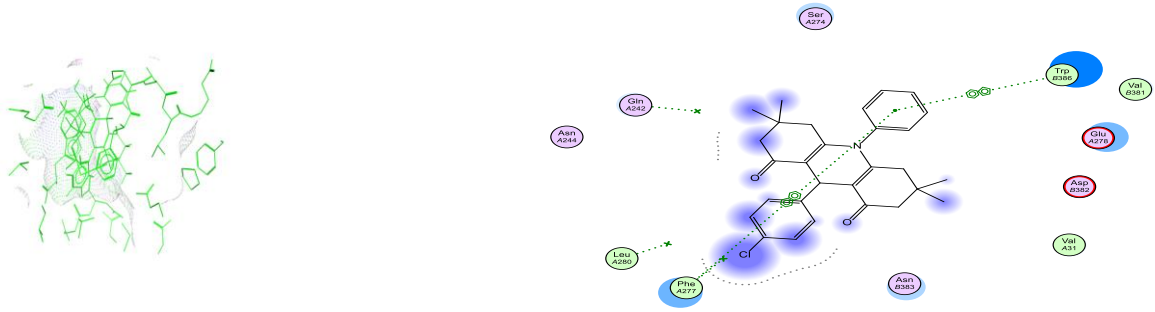

Figure 23. Showed 3D and 2D, interaction of C9/ 9-(4-chlorophenyl)-3,3,6,6-tetramethyl-10-phenyl-3,4,6,7,9,10-hexahydroacridine-1,8(2H,5H)-dione inside the active site of 5OM7 protein.

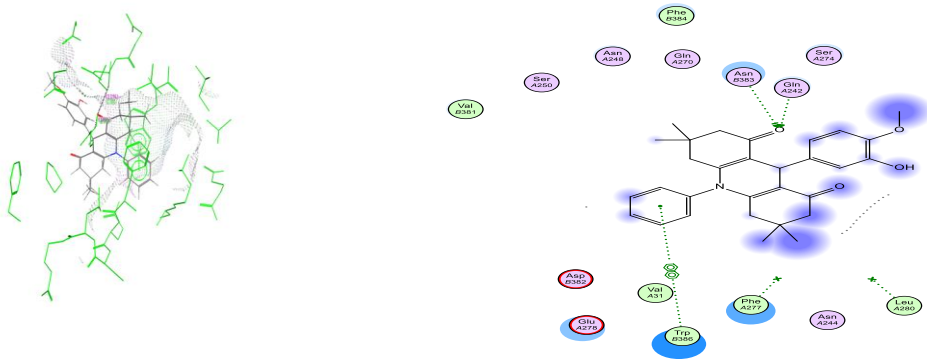

Figure 24. Showed 3D and 2D, interaction of C10/ 9-(3-hydroxy-4-methoxyphenyl)-3,3,6,6-tetramethyl-10-phenyl-3,4,6,7,9,10-hexahydroacridine-1,8(2H,5H)-dione inside the active site of 5OM7 protein.

العدد أربعون
تاريخ الإصدار: 2 – شباط – 2022 م
www.ajsp.net
ISSN: 2663-5798

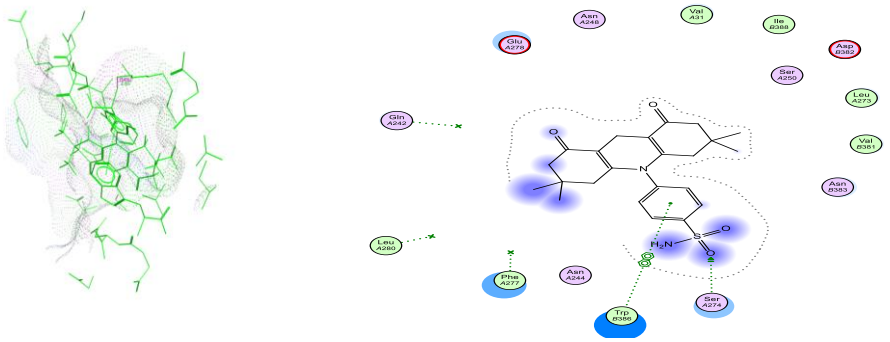

Figure 25. Showed 3D and 2D, interaction of C11/ 4-(3,3,6,6-tetramethyl-1,8-dioxo-2,3,4,5,6,7,8,9-octahydroacridin-10(1H)-yl)benzenesulfonamide inside the active site of 5OM7 protein.

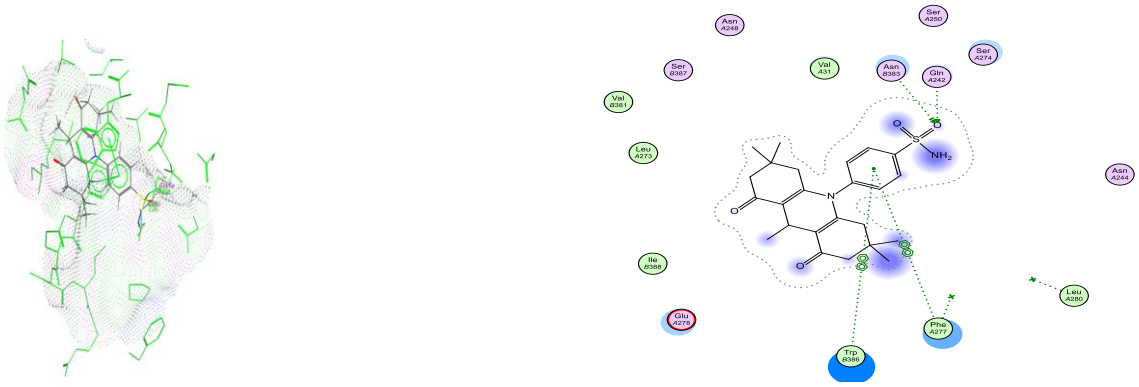

Figure 26. Showed 3D and 2D, interaction of C12/ 4-(3,3,6,6,9-pentamethyl-1,8-dioxo-2,3,4,5,6,7,8,9-octahydroacridin-10(1H)-yl)benzenesulfonamide inside the active site of 5OM7 protein.

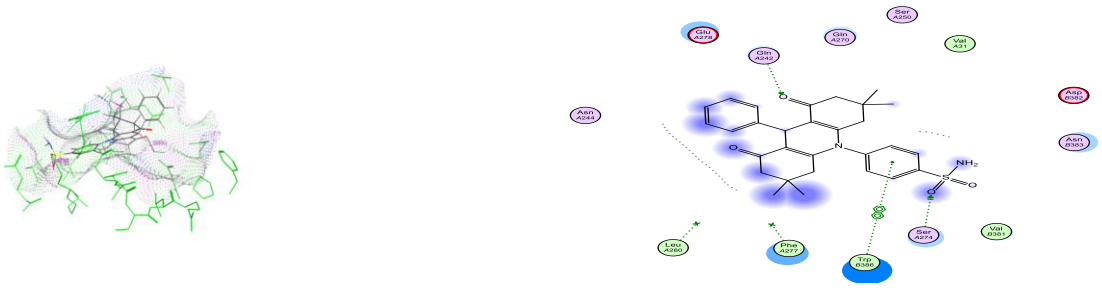

Figure 27. Showed 3D and 2D, interaction of C13/ 4-(3,3,6,6-tetramethyl-1,8-dioxo-9-phenyl-2,3,4,5,6,7,8,9-octahydroacridin-10(1H)-yl)benzenesulfonamide inside the active site of 5OM7 protein.

AJSP
المجلة العربية للنشر العلمي
العدد أربعون
تاريخ الإصدار: 2 – شباط – 2022 م
www.ajsp.net
ISSN: 2663-5798

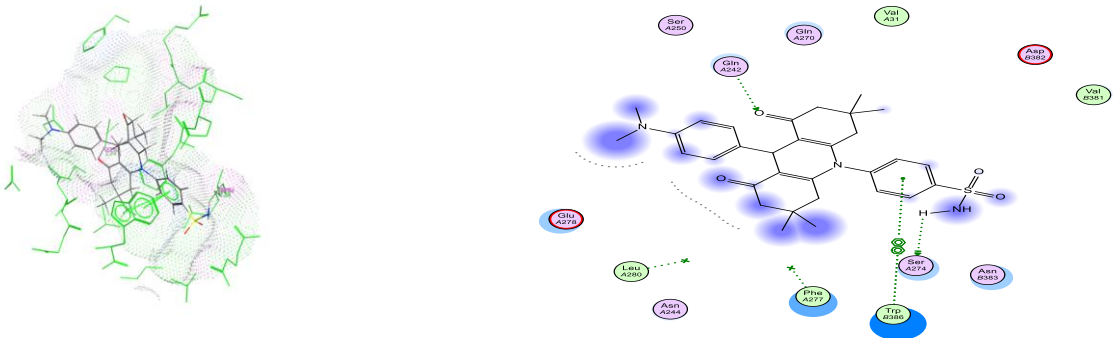

Figure 28. Showed 3D and 2D, interaction of C14/ 4-(9-(4-(dimethylamino)phenyl)-3,3,6,6-tetramethyl-1,8-dioxo-2,3,4,5,6,7,8,9-octahydroacridin-10(1H)-yl)benzenesulfonamide inside the active site of 5OM7 protein.

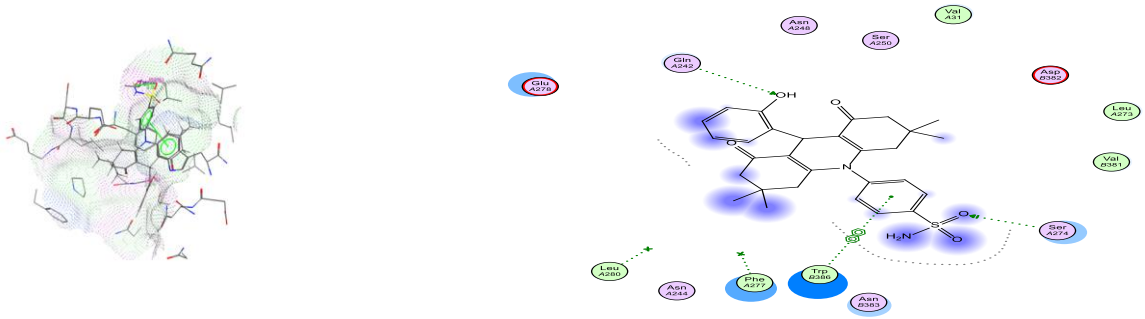

Figure 29. Showed 3D and 2D, interaction of C15/ 4-(9-(2-hydroxyphenyl)-3,3,6,6-tetramethyl-1,8-dioxo-2,3,4,5,6,7,8,9-octahydroacridin-10(1H)-yl)benzenesulfonamide inside the active site of 5OM7 protein.

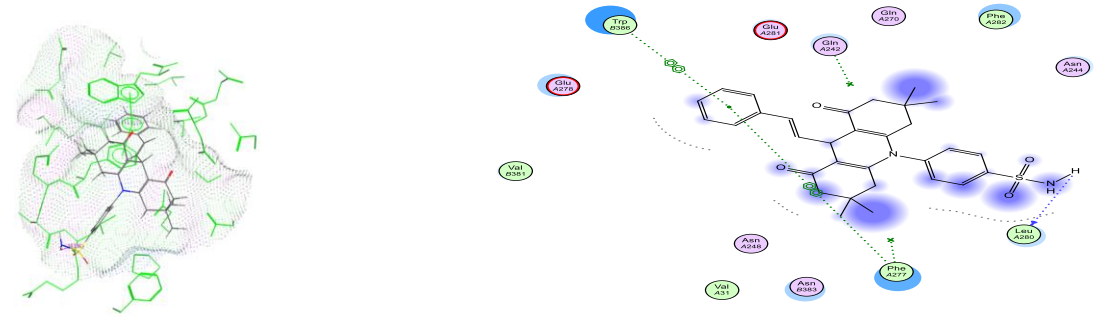

Figure 30. Showed 3D and 2D, interaction of C16/ (E)-4-(3,3,6,6-tetramethyl-1,8-dioxo-9-styryl-2,3,4,5,6,7,8,9-octahydroacridin-10(1H)-yl)benzenesulfonamide inside the active site of 5OM7 protein.

العدد أربعون
تاريخ الإصدار: 2 – شباط – 2022 م
www.ajsp.net
ISSN: 2663-5798

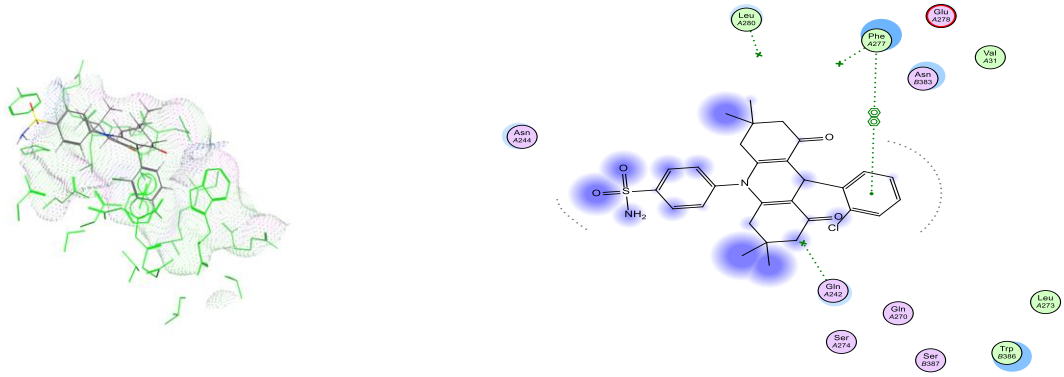

Figure 31. Showed 3D and 2D, interaction of C17/ 4-(9-(2-chlorophenyl)-3,3,6,6-tetramethyl-1,8-dioxo-2,3,4,5,6,7,8,9-octahydroacridin-10(1H)-yl)benzenesulfonamide inside the active site of 5OM7 protein.

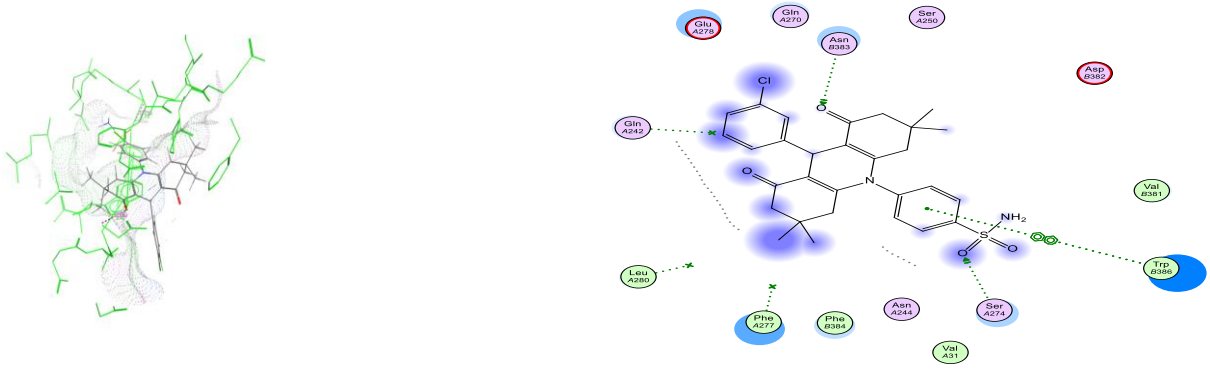

Figure 32. Showed 3D and 2D, interaction of C18/ 4-(9-(3-chlorophenyl)-3,3,6,6-tetramethyl-1,8-dioxo-2,3,4,5,6,7,8,9-octahydroacridin-10(1H)-yl)benzenesulfonamide inside the active site of 5OM7 protein.

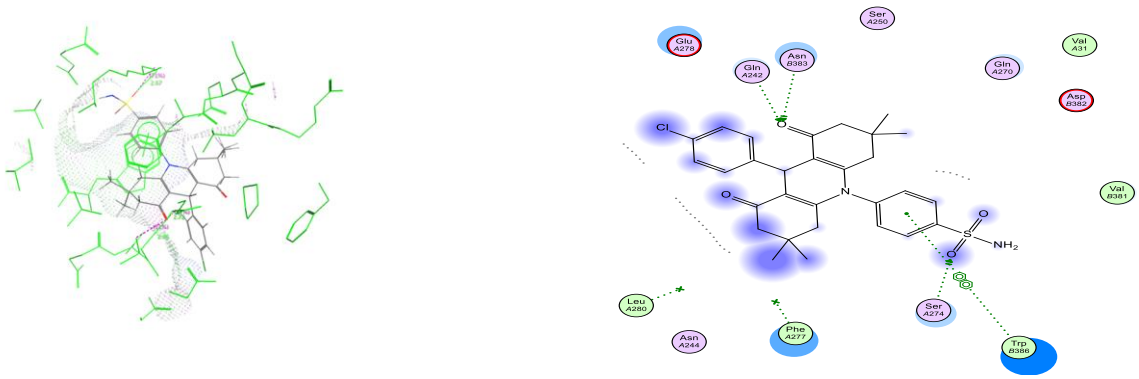

Figure 33. Showed 3D and 2D, interaction of C19/ 4-(9-(4-chlorophenyl)-3,3,6,6-tetramethyl-1,8-dioxo-2,3,4,5,6,7,8,9-octahydroacridin-10(1H)-yl)benzenesulfonamide inside the active site of 5OM7 protein.

العدد أربعون
تاريخ الإصدار: 2 – شباط – 2022 م
www.ajsp.net
ISSN: 2663-5798

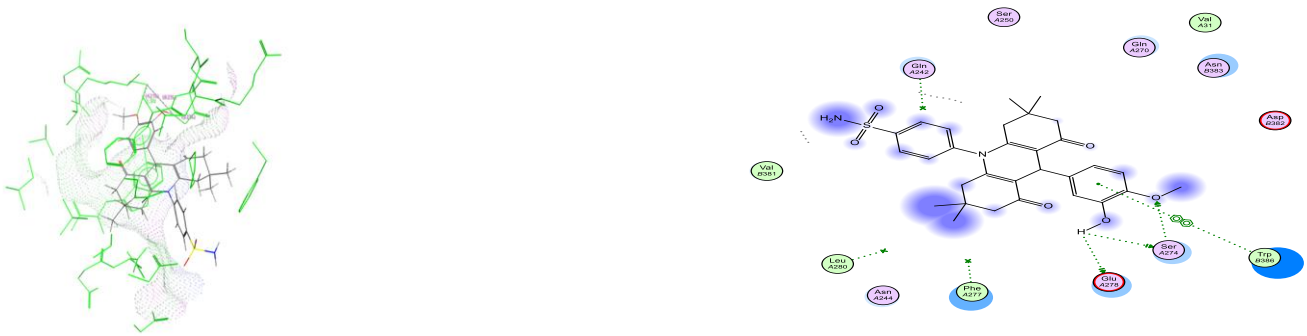

Figure 34. Showed 3D and 2D, interaction of C20/ 4-(9-(3-hydroxy-4-methoxyphenyl)-3,3,6,6-tetramethyl-1,8-dioxo-2,3,4,5,6,7,8,9-octahydroacridin-10(1H)-yl)benzenesulfonamide inside the active site of 5OM7 protein.

7. Conclusion

The QSAR modeling techniques involves the use of a significant number of statistical tools and hence requires a good knowledge of chemo metrics. The developed QSAR model can be furnish linear as well as nonlinear relationship between the response and chemical attributes through regression-based analyses. Since, quantitative mathematical relationships are established; validation of the model using a suitable statistical algorithm becomes essential to confirm the stability and predictivity of the model. The judgment for the choice of method depends upon a multitude of factors including the response to be modeled, the nature of the training set data, the descriptors used and also its numbers, and even the objective of the analysis.

The current work represents a powerful procedure for the preparation of N- substituted – 3, 3, 6, 6-tetramethylhexahydroacridine-1, 8- Dione derivatives . This general and efficient procedure offers several advantages including the usage of dual solvent system, wide scope of substrates, usage of very cheap and readily available Cetyl Trimethyl Ammonium Bromide (CTAB), a phase- transfer catalyst to the reaction mixtures as a catalyst, high yield and the facile separation of the products by simple filteration after washing with water. All of these points make this procedure as a very useful and practical alternative in the synthesis of these compounds.

References

1-Perkins, R., H. Fang, Tong, W., Welsh W.(2003) (Quantitative structure-activity relationship methods: Perspectives on drug discovery and toxicology." Environmental Toxicology and Chemistry: An International Journal **22**(8): 1666-1679.

2-Tropsha, A., P. Gramatica, P., and Gombar, V.K., (2003). "The importance of being earnest: validation is the absolute essential for successful application and interpretation of QSPR models." QSAR & Combinatorial Science **22**(1): 69-77.

3-Fujita, T., Iwasa J, andHansch, C,(1964). "A new substituent constant, π, derived from partition coefficients." Journal of the American Chemical Society **86**(23): 5175-51.80

4-Hansch, C., E. Lien, Steward, A.R., Anderson, S.M. and Bentley, D.L., (1968). "Structure-activity correlations in the metabolism of drugs." Archives of biochemistry and biophysics **128**(2): 319-330.

5-Bano, S., M. S. Alam, M.S., Javed.; K.; Dudeja, M.; Das, A.K., and Dhulap, A., (2015). "Synthesis, biological evaluation and molecular docking of some substituted pyrazolines and isoxazolines as potential antimicrobial agents." European journal of medicinal chemistry **95**: 96-103.

6- Ghorbani-Choghamarani, A., M. A. Zolfigol, A.R. Arbi, J.(2008). An Efficient Procedure for the Synthesis of Hantzsch 1, 4-Dihydropyridines Under Mild Conditions. Iran Journal of Chemical Society. 5, 96-99.

7- Leov, N. M. J. J. o. t. A. U. L. and L. Association (1965). Jacques le fataliste, poème parabolique.Jacques le Fataliste et Son maitre-Wikipedea. **2**.48-24 :(1)3

8-Wang, G.-W., Xiu, J.-J. Miao, L.B.,Wu,X.L.(2006). "Environmentally friendly and efficient synthesis of various 1, 4-dihydropyridines in pure water. Bull. Chem. Sos. JPn. **79**(3): 454-459.

9-Zhu, J. and H. Bienaymé (2006). Multicomponent reactions, John Wiley & Sons.

10-Mahama, O.,. Aboudramane, K, Kone Soleymane, and Collet Sylvain. (2020). Anticancer Activities and QSAR Study of Novel Agents with a Chemical Profile of Benzimidazolyl-Retrochalcone. Open Journal of Medicinal Chemistry. **10**(03): 113.

11- Jamalian, A.,Miri, R.; Firuzi, O.; Amini, M.; Moosavi-Movahedi, A.A.; and Shafiee, A. (2011). "Synthesis, cytotoxicity and calcium antagonist activity of novel imidazolyl derivatives of 1, 8-acridinediones." Journal of the Iranian Chemical Society **8**(4): 983-991.

12-Chai, T. and R. R. Draxler (2014). "Root mean square error (RMSE) or mean absolute error (MAE)." Geoscientific Model Development Discussions **7**(1): 1525-1534.

17-Yunta, M. (2017). It is important to compute intramolecular hydrogen bonding in drug design. Am. J. Model. Optim. **5**(1): 24-57.